Title	Acoustic waves at the interface of a pre-stressed incompressible elastic solid and a viscous fluid
Author(s)	Destrade, Michel
Publication Date	2006-11-10
Publication Information	OTTENIO, M., DESTRADE, M., OGDEN, R.W. (2007) 'Acoustic waves at the interface of a pre-stressed incompressible elastic solid and a viscous fluid'. International Journal of Non-Linear Mechanics, Special Issue in Honour of R.S. Rivlin, 42 :310-320.
Publisher	Elsevier
Link to publisher's version	http://dx.doi.org/10.1016/j.ijnonlinmec.2006.10.001
Item record	http://hdl.handle.net/10379/3170
DOI	http://dx.doi.org/http://dx.doi.org/10.1016/j.ijnonlinmec.2006.10.001

Acoustic waves at the interface of a pre-stressed incompressible elastic solid and a viscous fluid

M. Otténio, M. Destrade, R.W. Ogden

2006

Abstract

We analyze the influence of pre-stress on the propagation of interfacial waves along the boundary of an incompressible hyperelastic half-space that is in contact with a viscous fluid extending to infinity in the adjoining half-space.

One aim is to derive rigorously the incremental boundary conditions at the interface; this derivation is delicate because of the interplay between the Lagrangian and the Eulerian descriptions but is crucial for numerous problems concerned with the interaction between a compliant wall and a viscous fluid. A second aim of this work is to model the ultrasonic waves used in the assessment of aortic aneurysms, and here we find that for this purpose the half-space idealization is justified at high frequencies. A third goal is to shed some light on the stability behaviour in compression of the solid half-space, as compared with the situation in the absence of fluid; we find that the usual technique of seeking standing waves solutions is not appropriate when the half-space is in contact with a fluid; in fact, a correct analysis reveals that the presence of a viscous fluid makes a compressed neo-Hookean half-space slightly more stable.

For a wave travelling in a direction of principal strain, we obtain results for the case of a general (incompressible isotropic) strain-energy function. For a wave travelling parallel to the interface and in an arbitrary direction in a plane of principal strain, we specialize the analysis to the neo-Hookean strain-energy function.

1

1 Introduction

Seismic records show that underground rocks and ocean beds are subject to stress and strain and that surrounding fluids are viscous and under high pressures. Clinical ultrasonic measurements indicate that arteries can undergo large strains in service and are most sensitive to changes in blood pressure. Many moving and vibrating parts of automotive devices are made of loaded elastomers in contact with highly viscous fluids. These are a few examples of situations where it is crucial to model and understand the motions and the stability of the interface between a *deformed* elastic solid and a *viscous* fluid. Yet only a handful of studies can be found on the subject, especially when compared with the abundant literature on waves at the interface between an elastic solid and an *inviscid* fluid, which goes from the pioneering works of Galbrun [1], Cagniard [2], Scholte [3], and Biot [4] to the definitive treatment of the acoustoelastic effect by Sinha et al. [5]; see also Poirée [6] and Degtyar and Rohklin [7]. Waves at the interface between a viscous fluid and an *undeformed* isotropic elastic solid were examined by Vol'kenshtein and Levin [8] and the corresponding problem for an anisotropic elastic solid by Wu and Wu [9]. To the best of our knowledge, only Bagno, Guz, and their co-workers have studied the title problem (see, for example, [10], [11]). Their analytical treatment is, however, quite succinct and we therefore aim to shed new light on the problem by re-examining it on the basis of recent developments in the theory of small-amplitude waves, linearized in the neighbourhood of a finite, static, homogeneous deformation.

It turns out that one of the trickiest aspects of the study is the derivation of proper incremental boundary conditions at the interface because these are usually written in terms of the nominal stress in a deformed solid (Lagrangian formulation, Section 2) and in terms of the Cauchy stress in a fluid (Eulerian formulation, Section 3). These equations are combined in an appropriate way for a general interface in Section 4. We then specialize the analysis to principal wave propagation for an arbitrary (incompressible, isotropic) strain-energy function in Section 5. In the course of the analysis in Section 5, by way of application of the theory, we show that in respect of an abdominal aortic aneurysm it is appropriate to neglect the curvature and finite thickness for ultrasonic waves (10 MHz), i.e. to treat the aneurysm locally as a half-space. It also shown that it is not appropriate to use waves with a real frequency to study the stability of compressed solids in contact with a viscous fluid. Finally, in Section 6, by specializing to the neo-Hookean solid, we consider

the propagation of non-principal waves for both tension and compression of the half-space in order to illustrate the influence of the fluid.

2   Basic equations for the solid

For the solid material we denote by $\boldsymbol{F}$ the deformation gradient relating the stress-free reference configuration, denoted $\mathcal{B}_0$, to the finitely deforming configuration, denoted $\mathcal{B}$. This has the form $\boldsymbol{F} = \mathrm{Grad}\,\boldsymbol{x}$, where $\boldsymbol{x} = \boldsymbol{\chi}(\boldsymbol{X}, t)$ is the position vector in $\mathcal{B}$ at time t of a material point located at $\boldsymbol{X}$ in $\mathcal{B}_0$, $\boldsymbol{\chi}$ is the deformation mapping, and Grad is the gradient operator relative to $\mathcal{B}_0$.

We consider the material to be elastic with a strain-energy function, defined per unit volume, denoted by $W = W(\boldsymbol{F})$. Furthermore, we restrict attention to incompressible materials so that the constraint

$$\det \boldsymbol{F} = 1 \tag{2.1}$$

is in force. The nominal stress tensor, here denoted by $\boldsymbol{S}$, and the Cauchy stress tensor $\boldsymbol{\sigma}$ are then given by

$$\boldsymbol{S} = \frac{\partial W}{\partial \boldsymbol{F}} - p\boldsymbol{F}^{-1}, \quad \boldsymbol{\sigma} = \boldsymbol{F}\frac{\partial W}{\partial \boldsymbol{F}} - p\boldsymbol{I}, \tag{2.2}$$

where p is a Lagrange multiplier associated with the constraint (2.1) and $\boldsymbol{I}$ is the identity tensor.

The equation of motion is

$$\mathrm{Div}\,\boldsymbol{S} = \rho\ddot{\boldsymbol{x}}, \tag{2.3}$$

where Div is the divergence operator relative to $\mathcal{B}_0$, ρ is the mass density of the material, and a superposed dot signifies the material time derivative.

Next, we consider a small motion superimposed on the finite deformation. Let $\boldsymbol{u}(\boldsymbol{x}, t)$ be the displacement vector relative to $\mathcal{B}$ and $\boldsymbol{v}(\boldsymbol{x}, t) = \dot{\boldsymbol{u}}$ the associated particle velocity (the material time derivative of $\boldsymbol{u}$). Then, on taking the increment of equation (2.3) and thereafter changing the reference configuration from $\mathcal{B}_0$ to $\mathcal{B}$, we obtain

$$\mathrm{div}\,\boldsymbol{s} = \rho\ddot{\boldsymbol{u}} \equiv \rho\dot{\boldsymbol{v}}, \tag{2.4}$$

3

where $\boldsymbol{s}$ is the increment in $\boldsymbol{S}$ (referred to $\mathcal{B}$) and div the divergence operator relative to $\mathcal{B}$.

The (linearized) incremental version of the constitutive relation (2.2) is written

$$\boldsymbol{s} = \boldsymbol{\mathcal{A}}(\operatorname{grad}\boldsymbol{u}) + p(\operatorname{grad}\boldsymbol{u}) - \tilde{p}\boldsymbol{I}, \tag{2.5}$$

where $\boldsymbol{\mathcal{A}}$ is a fourth-order tensor of elastic moduli, grad is the gradient operator relative to $\mathcal{B}$, and $\tilde{p}$ is the increment in p. In component form, this is written

$$s_{ij} = \mathcal{A}_{ijkl}u_{l,k} + pu_{i,j} - \tilde{p}\delta_{ij}, \tag{2.6}$$

where $_{,k}$ denotes $\partial/\partial x_k$ and δ_{ij} is the Kronecker delta. In terms of W the components of $\boldsymbol{\mathcal{A}}$ are given by

$$\mathcal{A}_{ijkl} = F_{ip}F_{kq}\frac{\partial^2 W}{\partial F_{jp}\partial F_{lq}}. \tag{2.7}$$

For details of these derivations (in a slightly different notation) we refer to Dowaikh and Ogden [12].

We now consider the material to be isotropic, so that $W = W(\lambda_1, \lambda_2, \lambda_3)$ is a symmetric function of the principal stretches, $\lambda_1, \lambda_2, \lambda_3$ (the positive square roots of the principal values of $\boldsymbol{F}\boldsymbol{F}^T$, where ^{T} signifies the transpose), subject to the constraint

$$\lambda_1\lambda_2\lambda_3 = 1, \tag{2.8}$$

which follows from (2.1). Then, on noting that for an isotropic material $\boldsymbol{\sigma}$ is coaxial with $\boldsymbol{F}\boldsymbol{F}^T$ and specializing equation $(2.2)_2$, we obtain the principal Cauchy stresses (see, for example, Ogden [13])

$$\sigma_i = -p + \lambda_i W_i, \quad i = 1, 2, 3 \quad \text{(no sum over } i), \tag{2.9}$$

where $W_i = \partial W/\partial\lambda_i$, $i = 1, 2, 3$.

When referred to the same principal axes, the only non-zero components of $\boldsymbol{\mathcal{A}}$ are

$$\mathcal{A}_{iijj} = \lambda_i\lambda_j W_{ij}, \quad i, j \in \{1, 2, 3\}, \tag{2.10}$$

$$\mathcal{A}_{ijij} = \frac{\lambda_i W_i - \lambda_j W_j}{\lambda_i^2 - \lambda_j^2}\lambda_i^2, \quad i, j \in \{1, 2, 3\}, i \neq j, \tag{2.11}$$

$$\mathcal{A}_{ijji} = \mathcal{A}_{jiij} = \mathcal{A}_{ijij} - \lambda_i W_i, \quad i, j \in \{1, 2, 3\}, i \neq j, \tag{2.12}$$

4

where $W_{ij} = \partial^2 W / \partial \lambda_i \partial \lambda_j$. For subsequent convenience, we adopt the notations defined by

$$\gamma_{ij} = (\lambda_i W_i - \lambda_j W_j) \lambda_i^2 / (\lambda_i^2 - \lambda_j^2),$$
$$\beta_{ij} = (\lambda_i^2 W_{ii} + \lambda_j^2 W_{jj})/2 - \lambda_i \lambda_j W_{ij} + (\lambda_i W_j - \lambda_j W_i) \lambda_i \lambda_j / (\lambda_i^2 - \lambda_j^2), \quad (2.13)$$

noting that $\gamma_{ji} \lambda_i^2 = \gamma_{ij} \lambda_j^2$ and $\beta_{ji} = \beta_{ij}$.

2.1 The pre-stressed elastic half-space

We now consider $\mathcal{B}$ to be independent of time and to correspond to a pure homogeneous strain of a half-space defined by $x_2 \geqslant 0$. The half-space is maintained in this configuration so that its boundary $x_2 = 0$ is a principal plane of strain. We denote by x_1 and x_3 the other two principal directions of strain and by λ_1, λ_2, λ_3 the principal stretches in the x_1, x_2, x_3 directions, respectively. The corresponding principal Cauchy stresses are then as given by (2.9). In particular, the boundary $x_2 = 0$ is subject to a normal stress σ_2 and, after elimination of p, the other two principal Cauchy stresses are then given by

$$\sigma_1 = \sigma_2 + \lambda_1 W_1 - \lambda_2 W_2, \quad \sigma_3 = \sigma_2 + \lambda_3 W_3 - \lambda_2 W_2. \quad (2.14)$$

We are interested in the propagation of incremental (small amplitude) acoustic waves along the boundary plane $x_2 = 0$, in a direction making an angle θ with the principal direction x_1. The incremental velocity and nominal stress fields $\boldsymbol{v}$ and $\boldsymbol{s}$ are then considered as superimposed on this finite static configuration. We examine inhomogeneous time-harmonic plane waves of the form

$$\{\boldsymbol{v}, \boldsymbol{s}\}(x_1, x_2, x_3, t) = \{\hat{\boldsymbol{v}}(x_2), -(k/\omega)\hat{\boldsymbol{s}}(x_2)\} e^{ik(c_\theta x_1 + s_\theta x_3)} e^{-i\omega t}, \quad (2.15)$$

where we have introduced the notations $c_\theta = \cos\theta$, $s_\theta = \sin\theta$, k is the wave number, ω is the wave frequency, and $\hat{\boldsymbol{v}}$, $\hat{\boldsymbol{s}}$ are functions of x_2 only, such that

$$\hat{\boldsymbol{v}}(\infty) = \boldsymbol{0}, \quad \hat{\boldsymbol{s}}(\infty) = \boldsymbol{0}. \quad (2.16)$$

Using the results of Destrade et al. [14] (see also Chadwick [15]), we find that the incremental equations of motion can be written as a first-order differential system of six equations, namely

$$\boldsymbol{\xi}'(x_2) = ik\boldsymbol{N}\boldsymbol{\xi}(x_2), \quad (2.17)$$

5

where the notation $\boldsymbol{\xi}$ is defined by

$$\boldsymbol{\xi} = [\hat{v}_1, \hat{v}_2, \hat{v}_3, \hat{s}_{21}, \hat{s}_{22}, \hat{s}_{23}]^T, \tag{2.18}$$

and the 6×6 matrix $\boldsymbol{N}$ has the block structure

$$\boldsymbol{N} = \begin{bmatrix} \boldsymbol{N}_1 & \boldsymbol{N}_2 \\ \boldsymbol{N}_3 + \hat{\rho}\boldsymbol{I} & \boldsymbol{N}_1^T \end{bmatrix}, \tag{2.19}$$

in which the 3×3 matrices $\boldsymbol{N}_1$, $\boldsymbol{N}_2$, $\boldsymbol{N}_3$ are real and their components depend on the material parameters γ_{ij} and β_{ij} given in (2.13), and the notation $\hat{\rho} = \rho\omega^2/k^2$ has been introduced. Here $\boldsymbol{I}$ represents the 3×3 identity matrix.

Explicitly, $-\boldsymbol{N}_1$, $\boldsymbol{N}_2$, $-\boldsymbol{N}_3$ are

$$\begin{bmatrix} 0 & c_\theta(\gamma_{21} - \sigma_2)/\gamma_{21} & 0 \\ c_\theta & 0 & s_\theta \\ 0 & s_\theta(\gamma_{23} - \sigma_2)/\gamma_{23} & 0 \end{bmatrix}, \quad \begin{bmatrix} 1/\gamma_{21} & 0 & 0 \\ 0 & 0 & 0 \\ 0 & 0 & 1/\gamma_{23} \end{bmatrix}, \quad \begin{bmatrix} \eta & 0 & -\kappa \\ 0 & \nu & 0 \\ -\kappa & 0 & \mu \end{bmatrix}, \tag{2.20}$$

respectively, where

$$\begin{aligned} \eta &= 2c_\theta^2(\beta_{12} + \gamma_{21} - \sigma_2) + s_\theta^2\gamma_{31}, \\ \nu &= c_\theta^2[\gamma_{12} - (\gamma_{21} - \sigma_2)^2/\gamma_{21}] + s_\theta^2[\gamma_{32} - (\gamma_{23} - \sigma_2)^2/\gamma_{23}], \\ \mu &= c_\theta^2\gamma_{13} + 2s_\theta^2(\beta_{23} + \gamma_{23} - \sigma_2), \\ \kappa &= c_\theta s_\theta(\beta_{13} - \beta_{12} - \beta_{23} - \gamma_{21} - \gamma_{23} + 2\sigma_2). \end{aligned} \tag{2.21}$$

Equation (2.17) provides the general expression for the equations of motion, for arbitrary θ and W.

Now, in seeking a decaying partial-mode solution of the form

$$\boldsymbol{\xi}(x_2) = \mathrm{e}^{-ksx_2}\boldsymbol{\zeta}, \quad \Re(ks) > 0, \tag{2.22}$$

where $\boldsymbol{\zeta}$ is a constant vector and s an unknown scalar, we arrive at the eigenvalue problem $\boldsymbol{N}\boldsymbol{\zeta} = \mathrm{i}s\boldsymbol{\zeta}$. In general, the associated *propagation condition*, $\det(\boldsymbol{N} - \mathrm{i}s\boldsymbol{I}) = 0$, is a cubic in s^2 [16], where now $\boldsymbol{I}$ is the 6×6 identity matrix. Its analytical resolution is too cumbersome to be of practical interest, and so we specialize the general equations to the following, simpler, situations: (i) principal wave propagation ($\theta = 0$) for arbitrary W; (ii) non-principal wave propagation ($\theta \neq 0$) for the neo-Hookean material, for which

$$W = C(\lambda_1^2 + \lambda_2^2 + \lambda_3^2 - 3)/2, \tag{2.23}$$

6

where $C > 0$ is a constant (the shear modulus of the material in the reference configuration).

In Case (i), the equations of motion decouple the system

$$\begin{bmatrix} \hat{v}_3' \\ \hat{s}_{23}' \end{bmatrix} = \mathrm{i}k \begin{bmatrix} 1/\gamma_{21} & 0 \\ 0 & 1/\gamma_{23} \end{bmatrix} \begin{bmatrix} \hat{v}_3 \\ \hat{s}_{23} \end{bmatrix}, \tag{2.24}$$

(for which the trivial solution may be chosen) from a system of four differential equations for $\hat{v}_1$, $\hat{v}_2$, $\hat{s}_{21}$, $\hat{s}_{22}$. Hence, in this case, the wave is elliptically polarized, in the (x_1, x_2) plane. The corresponding propagation condition is a quadratic in s^2, which can be solved explicitly.

In Case (ii), we also find that the wave is two-partial, polarized in the plane containing the directions of propagation and attenuation (the saggital plane); there, the corresponding propagation condition involves the product of the factor $(s^2 - 1)$ and a term linear in s^2, which simplifies the analysis.

Before embarking on the details of these cases, we complete the description of the boundary-value problem by considering the behaviour of the wave in the fluid in the half-space $x_2 \leq 0$.

3 The fluid half-space

Adjoining the deformed solid half-space is a half-space $x_2 \leqslant 0$ filled with an incompressible viscous Newtonian fluid, for which all mechanical fields are denoted by a superscripted asterisk. In the static state the fluid is subject only to a hydrostatic stress $\boldsymbol{\sigma}^* = -P^* \boldsymbol{I}$, and by continuity of traction across the boundary $x_2 = 0$ we must have

$$- P^* = \sigma_2. \tag{3.1}$$

The constitutive law for the fluid associated with the motion is then written in terms of a superimposed Cauchy stress tensor, denoted here by $\boldsymbol{s}^*$ and given by

$$\boldsymbol{s}^* = -p^* \boldsymbol{I} + 2\mu^* \boldsymbol{D}^*, \quad \operatorname{tr} \boldsymbol{D}^* = 0, \tag{3.2}$$

where μ^* is the viscosity of the fluid,

$$\boldsymbol{D}^* = \frac{1}{2}[\operatorname{grad} \boldsymbol{v}^* + (\operatorname{grad} \boldsymbol{v}^*)^T], \tag{3.3}$$

$\boldsymbol{v}^*$ is the fluid velocity, and $p^* = p^*(\boldsymbol{x}, t)$.

We seek inhomogeneous waves with the same structure as in the solid, that is

$$\{\boldsymbol{v}^*, \boldsymbol{s}^*\}(x_1, x_2, x_3, t) = \{\hat{\boldsymbol{v}}^*(x_2), -(k/\omega)\hat{\boldsymbol{s}}^*(x_2)\}e^{ik(c_\theta x_1 + s_\theta x_3)}e^{-i\omega t}, \qquad (3.4)$$

where $\hat{\boldsymbol{v}}^*$, $\hat{\boldsymbol{s}}^*$ are functions of x_2 only, such that

$$\hat{\boldsymbol{v}}^*(-\infty) = \boldsymbol{0}, \quad \hat{\boldsymbol{s}}^*(-\infty) = \boldsymbol{0}. \qquad (3.5)$$

We find that the equations of motion, $\operatorname{div}\boldsymbol{s}^* = \rho^*\dot{\boldsymbol{v}}^*$ (where ρ^* is the mass density of the fluid), linearized in $\boldsymbol{v}^*$, can be cast as

$$\boldsymbol{\xi}^{*\prime}(x_2) = ik\boldsymbol{N}^*\boldsymbol{\xi}^*(x_2), \qquad (3.6)$$

where

$$\boldsymbol{\xi}^* = [\hat{v}_1^*, \hat{v}_2^*, \hat{v}_3^*, \hat{s}_{21}^*, \hat{s}_{22}^*, \hat{s}_{23}^*]^T, \qquad (3.7)$$

and the constant complex matrix $\boldsymbol{N}^*$ has the block structure

$$\boldsymbol{N}^* = \begin{bmatrix} \boldsymbol{N}_1^* & \boldsymbol{N}_2^* \\ \boldsymbol{N}_3^* + \hat{\rho}^*\boldsymbol{I} & \boldsymbol{N}_1^* \end{bmatrix}, \qquad (3.8)$$

$\boldsymbol{N}_1^*$, $\boldsymbol{N}_2^*$, $\boldsymbol{N}_3^*$ being real symmetric matrices, and the notation $\hat{\rho}^* = \rho^*\omega^2/k^2$ has been adopted. If we write $\hat{\mu}^* = \mu^*\omega$, then, respectively, $-\boldsymbol{N}_1^*$, $-i\hat{\mu}^*\boldsymbol{N}_2^*$, $-i\boldsymbol{N}_3^*/\hat{\mu}^*$ are

$$\begin{bmatrix} 0 & c_\theta & 0 \\ c_\theta & 0 & s_\theta \\ 0 & s_\theta & 0 \end{bmatrix}, \quad \begin{bmatrix} 1 & 0 & 0 \\ 0 & 0 & 0 \\ 0 & 0 & 1 \end{bmatrix}, \quad \begin{bmatrix} 4c_\theta^2 + s_\theta^2 & 0 & 3c_\theta s_\theta \\ 0 & 0 & 0 \\ 3c_\theta s_\theta & 0 & c_\theta^2 + 4s_\theta^2 \end{bmatrix}. \qquad (3.9)$$

Again, when we seek a decaying partial-mode solution, this time in the form

$$\boldsymbol{\xi}^*(x_2) = e^{ks^*x_2}\boldsymbol{\zeta}^*, \quad \Re(ks^*) > 0, \qquad (3.10)$$

where $\boldsymbol{\zeta}^*$ is a constant vector and s^* an unknown scalar, we end up with an eigenvalue problem, here $\boldsymbol{N}^*\boldsymbol{\zeta}^* = -is^*\boldsymbol{\zeta}^*$. The associated *propagation condition* is $\det(\boldsymbol{N}^* + is^*\boldsymbol{I}) = 0$, which here simplifies to

$$(s^{\star 2} - 1)(s^{\star 2} - 1 + i\epsilon)^2 = 0, \qquad (3.11)$$

with roots

$$\pm 1, \quad \pm\sqrt{1 - i\epsilon} \quad \text{(repeated)}, \qquad (3.12)$$

8

where $\epsilon = \hat{\rho}^*/\hat{\mu}^* = \rho^*\omega/(\mu^*k^2)$. The roots are independent of θ, as expected, because the fluid is isotropic. Corresponding to each of the four roots, there are four eigenvectors and therefore potentially four partial-modes. However, two of these must be discarded since their amplitudes do not decay with distance from the interface $x_2 = 0$. The two remaining modes form the basis for the general solution of the equations of motion that is needed for matching with the two-partial wave in the solid.

We now give the general boundary conditions at the deformed solid/viscous fluid interface.

4   The interface

In order to match the incremental tractions across the boundary it is necessary to work in terms of the Cauchy stress since the nominal stress is not defined inside the fluid. Towards this end we first calculate the incremental traction in the solid in terms of the Cauchy stress. Continuity of traction requires

$$\boldsymbol{S}^T\boldsymbol{N}\mathrm{d}A = \boldsymbol{\sigma}\boldsymbol{n}\mathrm{d}a = \boldsymbol{\sigma}^*\boldsymbol{n}\mathrm{d}a, \tag{4.1}$$

where $\mathrm{d}A$ and $\mathrm{d}a$ are the area elements in $\mathcal{B}_0$ and $\mathcal{B}$, respectively. Taking the increment of this and updating the reference configuration to $\mathcal{B}$ yields

$$\boldsymbol{s}^T\boldsymbol{n}\mathrm{d}a \equiv \tilde{\boldsymbol{\sigma}}\boldsymbol{n}\mathrm{d}a + \boldsymbol{\sigma}\widetilde{\boldsymbol{n}\mathrm{d}a} = \boldsymbol{s}^*\boldsymbol{n}\mathrm{d}a + \boldsymbol{\sigma}^*\widetilde{\boldsymbol{n}\mathrm{d}a}, \tag{4.2}$$

where a superposed tilde indicates an increment. Note that, after updating, $\boldsymbol{F} = \boldsymbol{I}$ and $\boldsymbol{S} = \boldsymbol{\sigma}$ in the configuration $\mathcal{B}$.

Now, according to Nanson's formula (applied to the boundary of the solid), we have $\boldsymbol{n}\mathrm{d}a = \boldsymbol{F}^{-T}\boldsymbol{N}\mathrm{d}A$, from which it follows, again after updating, that

$$\widetilde{\boldsymbol{n}\mathrm{d}a} = -(\mathrm{grad}\,\boldsymbol{u})^T\boldsymbol{n}\mathrm{d}a. \tag{4.3}$$

Hence, the incremental traction continuity condition can be written

$$\boldsymbol{s}^T\boldsymbol{n} \equiv [\tilde{\boldsymbol{\sigma}} - \boldsymbol{\sigma}(\mathrm{grad}\,\boldsymbol{u})^T]\boldsymbol{n} = [\tilde{\boldsymbol{\sigma}}^* - \boldsymbol{\sigma}^*(\mathrm{grad}\,\boldsymbol{u})^T]\boldsymbol{n}, \tag{4.4}$$

and we recall that $\boldsymbol{\sigma}^* = -P^*\boldsymbol{I}$.

Since $\boldsymbol{n}$ is in the x_2 direction for the considered half-space we may write the continuity condition in component form as

$$s_{2i} = s_{2i}^* + P^*u_{2,i}, \quad i = 1, 2, 3, \quad \text{on} \quad x_2 = 0. \tag{4.5}$$

9

Additionally, the velocity must be continuous, i.e.

$$v_i^* = v_i, \quad i = 1, 2, 3, \quad \text{on} \quad x_2 = 0. \tag{4.6}$$

In terms of the functions $\hat{\boldsymbol{v}}(x_2)$, $\hat{\boldsymbol{s}}(x_2)$ and their counterparts in the fluid, the boundary conditions become

$$\hat{v}_i^*(0) = \hat{v}_i(0), \quad i = 1, 2, 3, \tag{4.7}$$

and, noting that $v_i = -\mathrm{i}\omega u_i$,

$$\hat{s}_{12}^*(0) + c_\theta P^* \hat{v}_2(0) = \hat{s}_{21}(0), \quad \hat{s}_{32}^*(0) + s_\theta P^* \hat{v}_2(0) = \hat{s}_{23}(0), \tag{4.8}$$

and

$$\hat{s}_{22}^*(0) - \frac{\mathrm{i}}{k} P^* \hat{v}_2'(0) = \hat{s}_{22}(0). \tag{4.9}$$

5 Principal waves: no restriction on W

5.1 General solution in the solid

Here we take $\theta = 0$ and place no restriction on the form of W. When $\theta = 0$, the in-plane mechanical fields in the solid satisfy the equations of motion $\boldsymbol{\xi}' = \mathrm{i}k\boldsymbol{N}\boldsymbol{\xi}$, where now $\boldsymbol{\xi}(x_2) = [\hat{v}_1, \hat{v}_2, \hat{s}_{21}, \hat{s}_{22}]^T$ and

$$\boldsymbol{N} = \begin{bmatrix} 0 & -1 + \overline{\sigma}_2 & 1/\gamma_{21} & 0 \\ -1 & 0 & 0 & 0 \\ \hat{\rho} - \eta & 0 & 0 & -1 \\ 0 & \hat{\rho} - \nu & -1 + \overline{\sigma}_2 & 0 \end{bmatrix}, \tag{5.1}$$

with $\overline{\sigma}_2 = \sigma_2/\gamma_{21}$ and η and ν now reduced to

$$\eta = 2[\beta_{12} + \gamma_{21}(1 - \overline{\sigma}_2)], \quad \nu = \gamma_{12} + \gamma_{21}(1 - \overline{\sigma}_2)^2.$$

Here the propagation condition is a quadratic in s^2 [12] and given by

$$s^4 - 2\beta s^2 + \alpha^2 = 0, \tag{5.2}$$

where

$$2\beta = \frac{2\beta_{12} - \hat{\rho}}{\gamma_{21}}, \quad \alpha^2 = \frac{\gamma_{12} - \hat{\rho}}{\gamma_{21}}. \tag{5.3}$$

10

We recall that $\hat{\rho} = \rho\omega^2/k^2$. Formally, the roots of the quartic (5.2) are

$$\pm\sqrt{\beta + \sqrt{\beta^2 - \alpha^2}}, \quad \pm\sqrt{\beta - \sqrt{\beta^2 - \alpha^2}}. \tag{5.4}$$

We pause the analysis to highlight a particular feature of the present interface waves. Because the fluid is viscous, the wave number k is complex and so, therefore, are β and α. It follows that, in contrast to the purely elastic case [17], it is not clear *a priori* which two of these four roots are such that the decay condition Eq. $(2.22)_2$ is satisfied. Let s_1 and s_2 be two such roots. We note first that

$$s_1^2 + s_2^2 = 2\beta, \quad s_1^2 s_2^2 = \alpha^2, \tag{5.5}$$

and then, depending on which value in Eq. (5.4) they correspond to, one of the following four possibilities may arise:

$$
\begin{aligned}
s_1 s_2 &= \alpha, & s_1 + s_2 &= \sqrt{2(\beta + \alpha)}, \\
s_1 s_2 &= \alpha, & s_1 + s_2 &= -\sqrt{2(\beta + \alpha)}, \\
s_1 s_2 &= -\alpha, & s_1 + s_2 &= \sqrt{2(\beta - \alpha)}, \\
s_1 s_2 &= -\alpha, & s_1 + s_2 &= -\sqrt{2(\beta - \alpha)}.
\end{aligned} \tag{5.6}
$$

Now, the eigenvectors $\boldsymbol{\zeta}^1$ and $\boldsymbol{\zeta}^2$ associated with s_1 and s_2 are columns of the matrices adjoint to $\boldsymbol{N} - \mathrm{i}s_1\boldsymbol{I}$ and $\boldsymbol{N} - \mathrm{i}s_2\boldsymbol{I}$, respectively. Taking, for instance, the fourth column gives

$$\boldsymbol{\zeta}^i = [\mathrm{i}s_i, -1, -\gamma_{21}(1 + s_i^2 - \overline{\sigma}_2), -\mathrm{i}\gamma_{21}s_i(1 + 2\beta - s_i^2 - \overline{\sigma}_2)]^T, \quad i = 1, 2. \tag{5.7}$$

Finally, the general solution in the solid is

$$\boldsymbol{\xi}(x_2) = A_1 \mathrm{e}^{-ks_1 x_2}\boldsymbol{\zeta}^1 + A_2 \mathrm{e}^{-ks_2 x_2}\boldsymbol{\zeta}^2, \tag{5.8}$$

where A_1 and A_2 are constants.

5.2 General solution in the fluid

In the fluid, a two-partial solution is required for adequate matching at the interface. Taking $\theta = 0$ in Section 3, we find that the in-plane equations of motion are $\boldsymbol{\xi}^{*\prime} = \mathrm{i}k\boldsymbol{N}^*\boldsymbol{\xi}^*$, where now $\boldsymbol{\xi}^*(x_2) = [\hat{v}_1^*, \hat{v}_2^*, \hat{s}_{21}^*, \hat{s}_{22}^*]^T$ and

$$\boldsymbol{N}^* = \begin{bmatrix} 0 & -1 & \mathrm{i}/\hat{\mu}^* & 0 \\ -1 & 0 & 0 & 0 \\ 4\mathrm{i}\hat{\mu}^* + \hat{\rho}^* & 0 & 0 & -1 \\ 0 & \hat{\rho}^* & -1 & 0 \end{bmatrix}. \tag{5.9}$$

11

We assume that the wave propagates and is attenuated in the direction $x_1 \geqslant 0$. From Eq. (3.4) with $\theta = 0$, we see that these assumptions lead to

$$\Re(k) > 0, \quad \Im(k) > 0. \tag{5.10}$$

On the other hand, the wave is also attenuated with distance from the interface; it follows that we can discard the root -1 from Eq. (3.12) and retain the root $+1$. The choice to be made for the remaining two roots in Eq. (3.12) is not so clear cut and for the time being we call s^* the suitable root; hence s^* is such that

$$s^{*2} = 1 - i\epsilon, \quad \Re(ks^*) > 0. \tag{5.11}$$

Finally, the general solution in the fluid is

$$\boldsymbol{\xi}^*(x_2) = A_1^* e^{kx_2} \begin{bmatrix} i \\ 1 \\ -2i\hat{\mu}^* \\ -\hat{\mu}^*(1 + s^{*2}) \end{bmatrix} + A_2^* e^{ks^*x_2} \begin{bmatrix} is^* \\ 1 \\ -i\hat{\mu}^*(1 + s^{*2}) \\ -2\hat{\mu}^* s^* \end{bmatrix}, \tag{5.12}$$

where A_1^* and A_2^* are constants.

5.3 Dispersion equation for the interface wave

When we specialize the general boundary conditions (4.7), (4.8) and (4.9) to the present context, we find a linear homogeneous system of four equations for the four unknowns A_1, A_2, A_1^*, A_2^*, for which the associated determinant must be zero. After some manipulations, using Eq. (5.5), we find that

$$\begin{vmatrix} -s_1 & -s_2 & 1 & s^* \\ 1 & 1 & 1 & 1 \\ \gamma_{21}(1 + s_1^2) & \gamma_{21}(1 + s_2^2) & -2i\hat{\mu}^* & -i\hat{\mu}^*(1 + s^{*2}) \\ \gamma_{21}s_1(1 + s_2^2) & \gamma_{21}s_2(1 + s_1^2) & i\hat{\mu}^*(1 + s^{\star 2}) & 2i\hat{\mu}^* s^* \end{vmatrix} = 0. \tag{5.13}$$

We see at once that the normal load σ_2 does not appear explicitly in this equation. This feature highlights a major difference between a wave at the interface of a loaded solid half-space and a vacuum (Rayleigh wave) and a wave at the interface of a loaded solid half-space and a viscous fluid, as considered here; Chadwick and Jarvis [18] also noted this peculiarity for waves at the interface of two loaded solid half-spaces (Stoneley wave). Of course, σ_2 still plays an important role, in particular in the determination of the pre-stretch ratios and of the amplitudes of the tractions in the solid.

Once the determinant is expanded and the factors $(s_1 - s_2)(1 - s^*)$ are removed, we end up with the *exact dispersion equation*,

$$\gamma_{21}^2 \left[\frac{\gamma_{12} - \hat{\rho}}{\gamma_{21}} + \frac{2\beta_{12} + 2\gamma_{21} - \hat{\rho}}{\gamma_{21}} s_1 s_2 - 1 \right]$$
$$- \mathrm{i}\gamma_{21}\hat{\mu}^*[2(1 - s_1 s_2)(1 - s^*) + (s_1 + s_2)(1 + s^*)(s^* + s_1 s_2)]$$
$$+ \hat{\mu}^{*2}\left[\mathrm{i}\epsilon + (\mathrm{i}\epsilon - 4)\, s^*\right] = 0. \quad (5.14)$$

This equation is fully explicit because the terms $s_1 + s_2$, $s_1 s_2$, and s^* are given by Eqs. (5.6) and Eq. (5.11). Of course, as noted earlier, there are several possibilities for these terms, which generate in total eight different dispersion equations. In each case the resulting root(s) in k must be checked for validity against the propagation and decay conditions $(2.22)_2$, (5.10), and $(5.11)_2$, which we summarize here as

$$\Re(k) > 0, \quad \Im(k) > 0, \quad \Re(ks^*) > 0, \quad \Re(ks_1) > 0, \quad \Re(ks_2) > 0. \quad (5.15)$$

Notice that in the special case of solids whose strain-energy function W is such that $2\beta_{12} = \gamma_{12} + \gamma_{21}$, which includes the neo-Hookean solid (2.23), the biquadratic (5.2) factorizes as $(s^2 - 1)(s^2 - \alpha^2) = 0$. Hence $s_1 = 1$, $s_2 = \pm\alpha$, and the exact secular equation (5.14) simplifies accordingly, leading this time to four different exact dispersion equations.

5.4   Application: modelling of intravascular ultrasound

In recent years, intravascular ultrasound (IVUS) has proved to be a most promising tool of investigation for measuring and assessing abdominal aortic aneurysms. Its accuracy is as good as that of computed tomography (CT) scans and it has obvious non-radiative advantages [19], [20], [21]. We now apply the results of this section to an IVUS context.

First we recall that medical ultrasound imaging devices operate in the 1–10 MHz range; accordingly we take $\omega = 10^7$ Hz. We argue, and will check *a posteriori*, that at such high frequency the wavelength is small compared with the radius and thickness of an artery so that, as far as the propagation of localized waves is concerned, an aortic aneurysm can be modelled as a half-space. Here we take the axis of the artery along the x_1 direction and consider that the half-space $x_2 \leqslant 0$ is filled with blood.

For the solid, we use a strain-energy function devised by Raghavan and Vorp [22] to fit experimental data collected on uniaxial tension tests of aortic

aneurysms, namely

$$W = \mathcal{C}_1(\lambda_1^2 + \lambda_2^2 + \lambda_3^2 - 3) + \mathcal{C}_2(\lambda_1^2 + \lambda_2^2 + \lambda_3^2 - 3)^2, \qquad (5.16)$$

where, typically, $\mathcal{C}_1 = 0.175$ MPa, $\mathcal{C}_2 = 1.9$ MPa. We assume that the aneurysm corresponds to a region where the tissue undergoes a strain of 20%, and that the end-systolic blood pressure is high, $150\,\mathrm{mmHg}$ ($= 20\,\mathrm{kPa}$) say, so we take $\sigma_2 = 20\,\mathrm{kPa}$. We consider that the tissue is free to expand or contract in the x_3 direction with $\sigma_3 = 0$. From (2.14) we find the remaining stresses and strains. Summarizing, we have

$$\lambda_1 = 1.2, \quad \lambda_3 \simeq 0.908, \quad \sigma_1 \simeq 71.45\,\mathrm{kPa}, \quad \sigma_2 = 20\,\mathrm{kPa}, \quad \sigma_3 = 0, \quad (5.17)$$

with λ_2 calculated from the incompressibility condition. For the mass density, we take $\rho = 1000$ kg/m^3. For the blood, we use typical values of viscosity [23] and mass density [24]: $\mu^* = 3.5 \times 10^{-3}\,\mathrm{Ns/m^2}$, $\rho^* = 1050\,\mathrm{kg/m^3}$.

Here, the frequency ω is fixed as a real quantity *a priori*. We then replace k everywhere by $k = \omega S$, where $S = S^+ + \mathrm{i}S^-$ is the (complex) *slowness*, and the only unknown in the dispersion equation (5.14). The propagation and decay conditions (5.15) are satisfied and may be written as

$$\Re(S) > 0, \quad \Im(S) > 0, \quad \Re(Ss^*) > 0, \quad \Re(Ss_1) > 0, \quad \Re(Ss_2) > 0. \quad (5.18)$$

We find that the only qualifying root is

$$S = 2.721 \times 10^{-2} + 4.424 \times 10^{-4}\mathrm{i}, \qquad (5.19)$$

from which we deduce the phase speed $v = 1/S^+$, the damping factor $\gamma = S^-$, and the wavelength $\lambda_0 = 2\pi/(\omega S^+)$:

$$v = 36.75\,\mathrm{m/s}, \quad \gamma = 4.424 \times 10^{-4}\,\mathrm{m^{-1}}, \quad \lambda_0 = 23.1\,\mu\mathrm{m}. \qquad (5.20)$$

Then we plot the depth profiles of the wave. Its amplitude is the real part of $\boldsymbol{v}$ in the solid and of $\boldsymbol{v}^*$ in the fluid. Explicitly,

$$\Re(\boldsymbol{v}(x_1, x_2, t)) = \mathrm{e}^{-\gamma x_1} [\Re(\hat{\boldsymbol{v}}(x_2)) \cos \omega(x_1/v - t)].$$
$$-\Im(\hat{\boldsymbol{v}}(x_2)) \sin \omega(x_1/v - t)], \quad (5.21)$$

in the solid, and similarly for the fluid, for which $\boldsymbol{v}$ and $\hat{\boldsymbol{v}}$ are replaced by their asterisk counterparts. Clearly, the particle velocity is elliptically polarized,

14

and the lengths of the ellipse semi-axes decay with distance away from the interface and also with increasing x_1. Figure 1 shows the variations of the normal (continuous curve) and tangential (dotted curve) velocity components in the fluid ($x_2 \leqslant 0$) and in the solid ($x_2 \geqslant 0$), normalized with respect to $\hat{v}_2(0)$, as functions of x_2/λ_0. Note that the components are in phase quadrature. Note also, as is clear from the zooms shown in Figure 1, that the components are continuous across the interface, as expected, but their first derivatives are discontinuous. The wave is elliptically polarized near the interface; the major axis is normal to the interface and more than 12 times the length of the minor axis; the ellipse is described in a retrograde manner. This shape is carried through the depth of the solid whereas in the fluid, the wave becomes rapidly circularly polarized at a depth of about 0.06 wavelengths, and remains nearly so through the rest of the half-space. The localization is greater in the fluid than in the solid: the amplitude has almost vanished after one wavelength into the former and after five wavelengths in the latter. An aneurysm is typically 1 mm thick, which, with the numerical values used here, is more than 50 wavelengths; thus, the assumption of a semi-infinite solid is justified, as is the assumption of a flat interface (aneurysms are typically of diameter 5 cm).

Finally, we note that if the fluid is absent then the corresponding surface wave would travel with speed 40.734 m/s; hence the viscous fluid not only dampens the wave but also slows it down noticeably. Of course, blood flows in an artery, and creates shear deformation and stress in the solid. The influence of wall shear stress on the waves will be treated elsewhere.

5.5   Example: compressive stresses

Here we consider the behaviour of the elastic half-space (in contact with the viscous fluid) when it is compressed in the x_1 direction ($\lambda_1 < 1$). In their pioneering works, Green and Zerna [25] and Biot [26], [27] showed that when a highly elastic half-space with a free surface (no fluid contact) is compressed, a surface instability may develop. Focusing on neo-Hookean solids (2.23) they showed that the critical stretches are $\lambda_{\text{cr}} = 0.666$ for tangential equibiaxial compression ($\lambda_1 = \lambda$, $\lambda_2 = \lambda^{-2}$, $\lambda_3 = \lambda$), $\lambda_{\text{cr}} = 0.544$ for plane strain compression ($\lambda_1 = \lambda$, $\lambda_2 = \lambda^{-1}$, $\lambda_3 = 1$), and $\lambda_{\text{cr}} = 0.444$ for normal equibiaxial compression ($\lambda_1 = \lambda$, $\lambda_2 = \lambda^{-1/2}$, $\lambda_3 = \lambda^{-1/2}$). Theirs was a static stability analysis, later also included in a wider dynamical context by Flavin [28], Willson [29], Chadwick and Jarvis [30], Dowaikh and Ogden [12], and
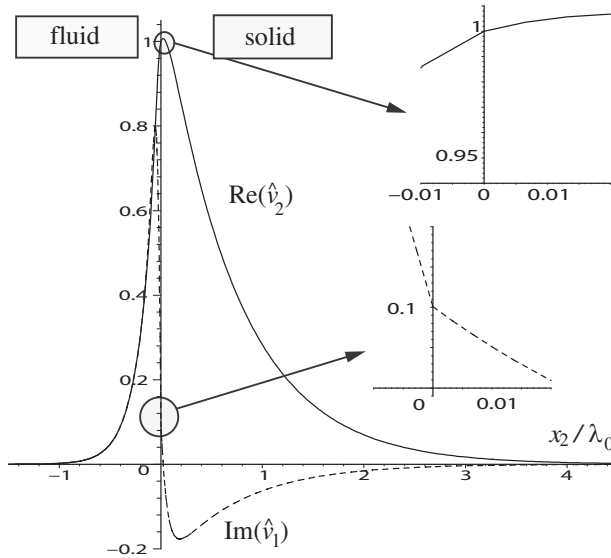
Figure 1: Depth profiles as functions of x_2/λ_0 of the velocity components of the acoustic wave: x_2 (normal) component – continuous curve; x_1 (tangential) component – dotted curve. The zooms show continuity of these components and discontinuity of their derivatives.

others. We now consider this problem.

A localized small-amplitude wave propagates over the free surface of a deformed Mooney-Rivlin or neo-Hookean half-space with normalized squared speed $\rho v^2/\gamma_{12} = 1 - \sigma_0^2 \lambda_2^2/\lambda_1^2$, where σ_0 is the real root of $\sigma^3 + \sigma^2 + 3\sigma - 1 = 0$ ($\sigma_0 = 0.2956$). Clearly, in the examples of plane strain and equi-biaxial strain above, the squared wave speed increases when λ increases and decreases when λ decreases. At $\lambda = 1$ there is no pre-strain and $\rho v^2/C = 0.9126$, the value found by Lord Rayleigh [31] for isotropic incompressible linearly elastic solids. As $\lambda \to \infty$, the squared wave speed tends to the squared wave speed γ_{12}/ρ of a transverse bulk wave. As λ decreases, there is a critical stretch λ_{cr} at which the squared speed is zero and below which $v^2 < 0$. Since the wave time dependence is of the form $\mathrm{e}^{\mathrm{i}k(x_1 - vt)}$, with $k > 0$, it follows that the amplitude grows without bound in time when $\lambda < \lambda_{\mathrm{cr}}$, and that the surface becomes unstable (at least, in the linearized theory). It is therefore appropriate to ask what happens when the compressed half-space is in contact with a viscous fluid.

Bagno and co-workers addressed this question in a series of articles (see

the review by Bagno and Guz [11] and references therein). For a neo-Hookean solid they found that the wave speed drops to zero when $\lambda = 0.544$ in plane strain compression and when $\lambda = 0.444$ in normal equi-biaxial compression, that is at the *same* critical stretches as for surface (solid/vacuum) instability, irrespective of the viscous fluid characteristics. On the other hand, Bagno and Guz [10] find that the wave speed falls to zero at a critical stretch that *does* depend upon the viscosity of the fluid. To address this disparity, we now compute the speed of the interfacial wave when the half-space is in compression.

In order to minimize the number of parameters, we use the neo-Hookean solid, with W given by (2.23). We take a normal equi-biaxial pre-strain ($\lambda_1 = \lambda$, $\lambda_2 = \lambda^{-1/2}$, $\lambda_3 = \lambda^{-1/2}$) and, following Bagno and Guz, we take the frequency ω to be real. A dimensional analysis of the resulting dispersion equation shows that (5.14) now depends on just three non-dimensional parameters: a measure of the pre-strain, λ; a measure of the dynamic viscosity of the fluid compared with the shear modulus of the solid, $\mu^* \omega / C$; and the ratio of the densities, ρ^* / ρ. Once these quantities are specified, the dispersion equation may be solved for the non-dimensional complex unknown x defined by

$$x := \sqrt{\frac{\rho}{\gamma_{12}}} \frac{\omega}{k} = \sqrt{\frac{\rho}{C \lambda^2}} S^{-1}, \tag{5.22}$$

where S is the (complex) scalar slowness. The dispersion equation can now be solved numerically for x, and the interfacial wave speed, normalized with respect to the transverse bulk shear wave speed in the deformed solid, is $c = \Re(1/x)$.

For Figure 2(a), we fix ρ^* / ρ at 1.0 and we take in turn $\mu^* \omega / C = 0.2$, 0.04, 0.02. The first choice ($\rho^* / \rho = 1.0$, $\mu^* \omega / C = 0.2$) is roughly that obtained for the blood/artery interface of the previous section with $\mathcal{C}_1 = C$ and $\mathcal{C}_2 = 0$. We see clearly that as $\mu^* \omega / C$ decreases the wave speed decreases towards zero as λ tends to 0.444, the critical compression stretch for the solid/vacuum interface (the thick curve gives the solid/vacuum interface wave speed). We find that in the extension to moderate compression range, the solid/fluid interface wave speed is significantly lower than the solid/vacuum wave speed. In the strongly compressive range (as $\lambda \to 0.444$), the speed plot dips towards zero, and dips further as $\mu^* \omega / C$ decreases, *without ever reaching that value*; the plot gets close to the plot for the solid/vacuum interface wave speed as λ decreases, but then crosses it, and the fluid/solid interface wave speed
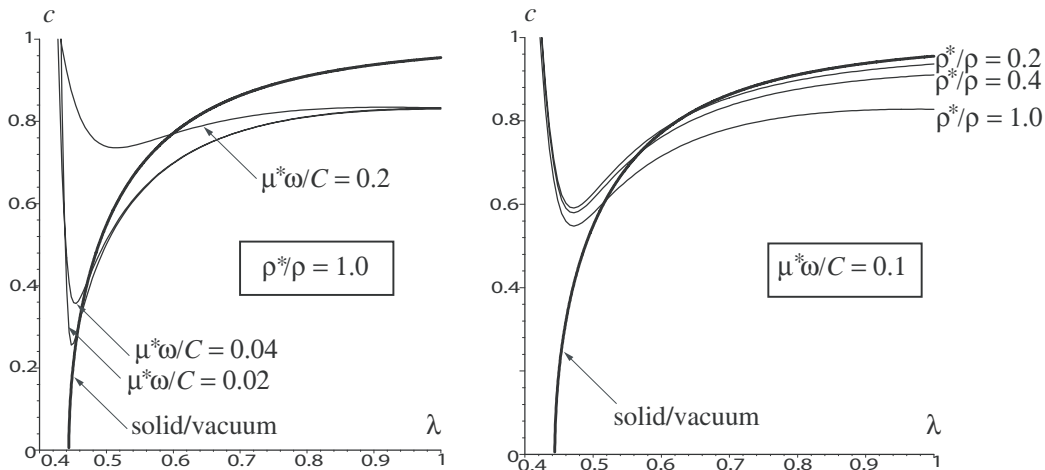
Figure 2: Normalized wave speed for a neo-Hookean solid under normal equibiaxial pre-strain and a viscous fluid: (a) $\rho^*/\rho = 1.0$ and $\mu^*\omega/C = 0.2$, 0.04, 0.02; (b) $\rho^*/\rho = 1.0$, 0.4, 0.2 and $\mu^*\omega/C = 0.1$. The thick curves are for an unloaded solid half-space.

increases again. Note that we checked the validity of the solution at all compressive stretches using (5.18).

For Figure 2(b), we fixed $\mu^*\omega/C$ at 1.0 and took $\rho^*/\rho = 0.1, 0.05, 0.01$. In the extension to moderate compression range, the plot for the solid/fluid interface wave speed gets closer to that for the solid/vacuum interface wave speed as ρ^*/ρ decreases. In the strongly compressive range, similar comments to those made for Figure 2(a) apply.

The conclusion is that as both $\mu^*\omega/C$ and ρ^*/ρ tend to zero, the speed tends to zero when the stretch tends to the critical compression stretch of the solid/vacuum surface instability. This is to be expected because this double limit corresponds to the vanishing of the fluid. However, as emphasized earlier, the speed never reaches the zero limit and the bifurcation criterion is therefore never met. For instance, the typical values used by Bagno and co-workers [11] put $\mu^*\omega/C$ at about 0.0002 and ρ^*/ρ as low as 0.1, giving c smaller than 10^{-4}, but not zero. In effect a localized damped wave exists for the whole compressive range, with speed values starting below the solid/vacuum interface wave speed in the moderate compressive range, reaching a minimum (above the solid/vacuum interface wave speed) as λ approaches 0.444, and then rising rapidly to infinity as λ decreases below 0.444.

This result suggests that when a neo-Hookean half-space is in contact with a viscous fluid it becomes completely stable. This, however, is an incorrect deduction, because it is based on special motions, for which the frequency ω is assumed real. Other motions might be unstable, as is illustrated below.

We now take the wave number k to be real ($k > 0$) and let the speed v be complex,

$$k > 0, \qquad v = v^+ + \mathrm{i}v^-, \tag{5.23}$$

so that the motion is now proportional to $\mathrm{e}^{kv^- t}\mathrm{e}^{\mathrm{i}k(x_1 - v^+ t)}$. Clearly in this case, the conditions for a stable, localized wave, propagating in the $x_1 > 0$ direction, are

$$\Re(v) \geqslant 0, \quad \Im(v) \leqslant 0, \quad \Re(s^*) > 0, \quad \Re(s_1) > 0, \quad \Re(s_2) > 0. \tag{5.24}$$

(note that $\Re(s_1) > 0$ is automatically satisfied in a neo-Hookean solid, because $s_1 = 1$).

Then, an analysis of the dispersion equation (5.14), in the case of a neo-Hookean solid with normal equi-biaxial pre-strain, reveals three non-dimensional quantities: λ, $\mu^* k/\sqrt{\rho C}$, and ρ^*/ρ. Once they are specified, we solve the dispersion equation for the non-dimensional quantity x defined as

$$x := \sqrt{\frac{\rho}{\gamma_{12}}}\frac{\omega}{k} = \sqrt{\frac{\rho}{C\lambda^2}}v. \tag{5.25}$$

The interfacial wave speed, normalized with respect to the transverse bulk shear wave speed in the deformed solid, is $c = \Re(x)$.

For Figure 3, we take $\rho^*/\rho = 1.0$, and $\mu^* k/\sqrt{\rho C} = 0.2, 0.002$ in turn, and we plot v against λ in the compressive range. We find that at a compressive stretch close to the critical compressive stretch of surface stability for the solid/vacuum interface, the normalized speed c drops to zero. From the figure it is not clear that the values of λ at this point are different for 0.2 and 0.002, but the zoom in Figure 3 shows, however, that the value of the compressive stretch at which $c = 0$ depends on the material parameters. For comparison, the curve corresponding to $\mu^* k/\sqrt{\rho C} = 1$ is also shown. We emphasize that the situation at $c = 0$ does not correspond to a static solution of the equations of motion (which would be impossible in the fluid), but to a non-propagating damped motion, proportional to $\mathrm{e}^{kv^- t}\mathrm{e}^{\mathrm{i}kx_1}$. Moreover, this situation does not correspond to an instability because at that point, and a bit beyond, the requirements (5.24) still hold. For instance, in the case
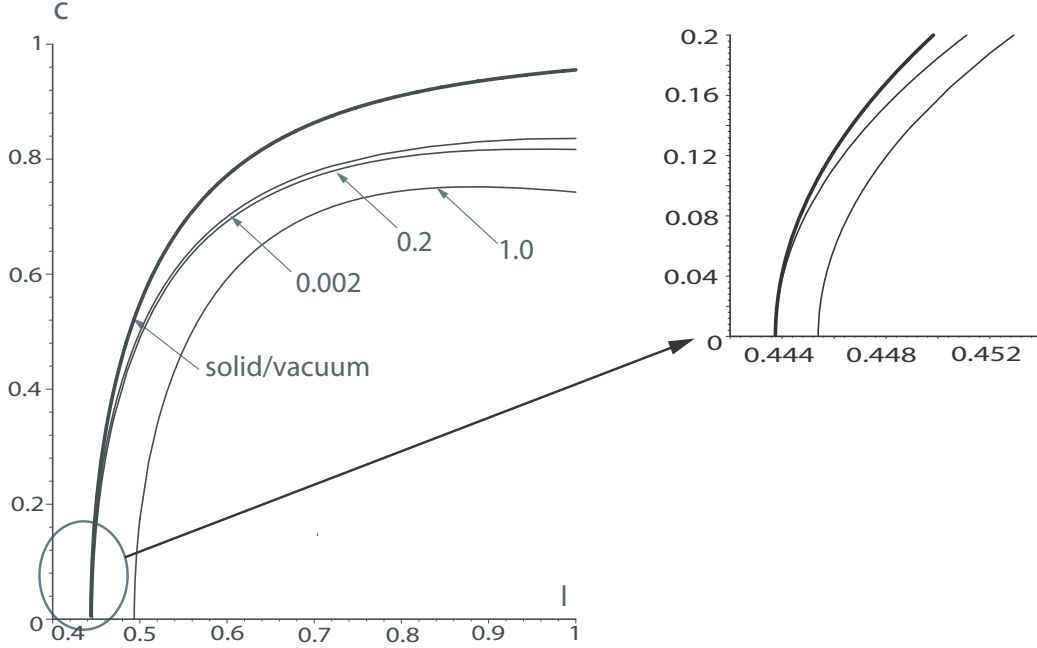
Figure 3: Normalized wave speed for a neo-Hookean solid under normal equi-biaxial pre-strain and a viscous fluid with $\rho^*/\rho = 1.0$ and $\mu^* k/\sqrt{\rho C} = 0.2, 0.002, 1$ (indicated by the arrows) for the compressive range $0.4 < \lambda < 1$. The zoom shows the details for $\mu^* k/\sqrt{\rho C} = 0.2, 0.002$ for $0.442 < \lambda < 0.445$ range. The thick curve corresponds to the solid half-space with no fluid loading.

$\rho^*/\rho = 1.0$, $\mu^* k/\sqrt{\rho C} = 0.2$, the speed drops to zero at $\lambda \simeq 0.44539$ but there still exist non-propagating, localized motions for $\lambda > 0.42212$. Beyond that stretch value, however, all solutions of the considered type grow unboundedly with time and/or with space, indicating instability. From this example we see that the viscous load stabilizes slightly the solid half-space, because it can now be compressed by an extra 2%, from 0.444 to 0.422.

6   Non-principal wave: neo-Hookean solid

In this section we consider that the solid half-space is a deformed neo-Hookean material, with strain-energy function given by Eq. (2.23). For this material, Flavin [28] noticed that Rayleigh waves are plane-polarized for any

20

direction of propagation in a principal plane; see [32], [33]. Chadwick and Jarvis [18] showed the same result for Stoneley waves. Indeed, we now show that the saggital motion is *always decoupled* from the 'anti-saggital' motion, for any θ and any type of (bulk or interfacial) inhomogeneous wave.

First, we note that for neo-Hookean bodies, the parameters γ_{ij} and β_{ij} have the simple expressions

$$\gamma_{ij} = C\lambda_i^2, \quad \beta_{ij} = C(\lambda_i^2 + \lambda_j^2)/2. \tag{6.1}$$

It follows that the matrices $\boldsymbol{N}_1$, $\boldsymbol{N}_2$, $\boldsymbol{N}_3$, given by Eq. (2.20), are greatly simplified. Next, we recall that the direction of propagation and the normal to the interface define the *saggital plane*, with unit normal $[-s_\theta, 0, c_\theta]^T$. Now consider the new unknown functions w_i, t_{2i} $(i = 1, 2, 3)$, defined by

$$w_i = \Omega_{ij}\hat{v}_j, \quad t_{2i} = \Omega_{ij}\hat{s}_{2j}, \tag{6.2}$$

where

$$\Omega_{ij} = \begin{bmatrix} c_\theta & 0 & s_\theta \\ 0 & 1 & 0 \\ -s_\theta & 0 & c_\theta \end{bmatrix}. \tag{6.3}$$

Some algebraic manipulations reveal that the equations of motion (2.17), written for w_i, t_{2i}, decouple the 'anti-saggital' motion $[w_3, t_{23}]$ from its saggital counterpart. For the latter we find

$$[w_1', w_2', t_{21}', t_{22}']^T = \mathrm{i}k\boldsymbol{N}[w_1, w_2, t_{21}, t_{22}]^T, \tag{6.4}$$

with $\boldsymbol{N}$ in the form (5.1), where now

$$\begin{array}{ll} \eta = C(c_\theta^2\lambda_1^2 + s_\theta^2\lambda_3^2 + 3\lambda_2^2) - 2\sigma_2, & \gamma_{21} = C\lambda_2^2, \\ \nu = C(c_\theta^2\lambda_1^2 + s_\theta^2\lambda_3^2) + C\lambda_2^2(1 - \overline{\sigma}_2)^2, & \overline{\sigma}_2 = \sigma_2/(C\lambda_2^2). \end{array} \tag{6.5}$$

A search for partial-mode solutions in the form $[w_1, w_2, t_{21}, t_{22}]^T = \boldsymbol{\zeta}\mathrm{e}^{-ksx_2}$, where $\boldsymbol{\zeta}$ is a 4-component constant vector, leads to an eigenvalue problem. The associated characteristic equation is the propagation condition

$$(s^2 - 1)[C\lambda_2^2 s^2 - C(c_\theta^2\lambda_1^2 + s_\theta^2\lambda_3^2) + \hat{\rho}] = 0, \tag{6.6}$$

with roots $s = -1$, which is discarded because it does not lead to a decaying wave,

$$s_1 = 1, \quad s_2 = \pm\sqrt{[C(c_\theta^2\lambda_1^2 + s_\theta^2\lambda_3^2) - \hat{\rho}]/(C\lambda_2^2)}. \tag{6.7}$$

The analysis leading to the derivation of the dispersion equation is by and large the same as that conducted for the principal wave in Section 5. The end result is that the dispersion equation is again (5.13), where now s_1 and s_2 are given by the expressions above, and γ_{21} is replaced by $C\lambda_2^2$, but the other quantities remain unchanged.

As an illustration, we take the same numerical values as in Section 5.4, but with $\mathcal{C}_2 = 0$ in (5.16). Hence the solid is neo-Hookean with $C = 0.175\,\mathrm{MPa}$ and $\rho = 1000\,\mathrm{kg/m^3}$. It is under the pre-stress $\sigma_2 = 20\,\mathrm{kPa}$, $\sigma_3 = 0$. The fluid has Newtonian viscosity $\mu^* = 3.5 \times 10^{-3}\,\mathrm{Ns/m^2}$, and mass density $\rho^* = 1050\,\mathrm{kg/m^3}$. The frequency is $\omega = 10^7\,\mathrm{Hz}$. In turn, we take the solid to be compressed by 20% in the x_1 direction (so that $\lambda_1 = 0.8$ and then $\lambda_2 \simeq 1.131$, $\lambda_3 \simeq 1.105$), to be unstretched in the x_1 direction (so that $\lambda_1 = 1$, and $\lambda_2 \simeq 1.014$, $\lambda_3 \simeq 0.986$), and to be under an extension of 20% in the x_1 direction (so that $\lambda_1 = 1.2$, and $\lambda_2 \simeq 0.929$, $\lambda_3 \simeq 0.897$).

Figure 4 shows the dependence of the interfacial wave speed $v^+ = \Re(\omega/k)$ on the angle of propagation θ. When the solid is almost unstrained, the speed hardly varies with the angle; when it is strained to $\pm 20\%$, the induced anisotropy causes speed changes of more than $\pm 25\%$ in some directions. The figure also shows clearly that the wave travels at its fastest in the direction of greatest stretch, and at its slowest in the direction of greatest compression, indicating that it could be used for the acoustic determination of these directions.

References

[1] H. Galbrun, *Propagation d'une Onde Sonore dans l'Atmosphère et Théorie des Zones de Silence.* Gauthier-Villars, Paris (1931).

[2] L. Cagniard, *Réflexion et Eéfraction des Ondes Sismiques Progressives.* Gauthier-Villars, Paris (1939)

[3] J.G. Scholte, On the Stoneley wave equation. *Proc. K. Ned. Akad. Wet.* **45**, Pt. 1: 20, Pt. 2: 159 (1942).

[4] M.A. Biot, The interaction of Rayleigh and Stoneley waves in the ocean bottom. *Bull. Seism. Soc. Am.* **42**, 81 (1952).

[5] B.K. Sinha, S. Kostek, and A.N. Norris, Stoneley and flexural modes in a pressurized borehole. *J. Geophys. Res.* **100**, 22375 (1995).
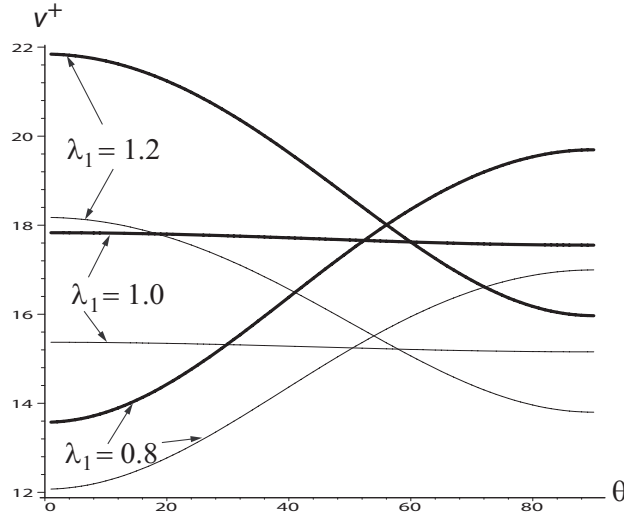
Figure 4: Influence of propagation angle θ on the speed v^+ of a wave at the interface between a viscous fluid and a deformed neo-Hookean solid (thin curves). The thick curves represent the wave speed in the absence of fluid loading.

[6] B. Poirée, Les équations de l'acoustique linéaire et non-linéaire dans un écoulement de fluide parfait. *Acustica* **57**, 5 (1985).

[7] A.D. Degtyar and S.I. Rokhlin, Stress effect on boundary conditions and elastic wave propagation through an interface between anisotropic media. *J. Acoust. Soc. Am.* **104**, 1992 (1998).

[8] M.M. Vol'kenshtein and V.M. Levin, Structure of a Stoneley wave at an interface between a viscosus fluid and a solid. *Sov. Phys. Acoust.* **34**, 351 (1987).

[9] T.-T. Wu and T.Y. Wu, Surface waves in coated anisotropic medium loaded with viscous liquid. *J. Appl. Mech.* **67**, 262 (2000).

[10] A.M. Bagno and A.N. Guz, Stonely waves on the contact boundary between a prestressed incompressible rigid half-space and a viscous compressible fluid. *Mech. Solids* **22**, 102 (1987).

[11] A.M. Bagno and A.N. Guz, Elastic waves in prestressed bodies interacting with a fluid. *Int. Applied Mech.* **33**, 435 (1997).

[12] M.A. Dowaikh and R.W. Ogden, On surface waves and deformations in a pre-stressed incompressible elastic solid. *IMA J. Appl. Math.* **44**, 261 (1990).

[13] R.W. Ogden, *Non-Linear Elastic Deformations.* Dover, New York (1997).

[14] M. Destrade, M. Otténio, A.V. Pichugin, and G.A. Rogerson, Non-principal surface waves in deformed incompressible materials. *Int. J. Eng. Sci.* **42**, 1092 (2005).

[15] P. Chadwick, The application of the Stroh formalism to prestressed elastic media. *Maths. Mech. Solids* **97**, 379 (1997).

[16] G.A. Rogerson and K.J. Sandiford, Harmonic wave propagation along a non-principal direction in a pre-stressed elastic plate. *Int. J. Eng. Sci.* **37**, 1663 (1999).

[17] M.A. Dowaikh and R.W. Ogden, Interfacial waves and deformations in pre-stressed elastic media. *Proc. Roy. Soc. Lond. A* **433**, 313 (1991).

[18] P. Chadwick and D.A. Jarvis, Interfacial waves in a pre-strained neo-Hookean body I. Biaxial states of strain. *Q. J. Mech. Appl. Math.* **32**, 387 (1979).

[19] F.A. Lederle, S.E. Wilson, G.R. Johnson, D.B. Reinke, F.N. Littooy, C.W. Acher, L.M. Messina, D.J. Ballard, and H.J. Ansel, Variability in measurement of abdominal aortic aneurysms. *J. Vasc. Surg.* **21**, 945 (1995).

[20] Y.G. Wolf, L.B. Johnson, B.B. Hill, G.D. Rubin, T.J. Fogarty, and C.K. Zarins, Duplex ultrasound scanning versus computed tomographic angiography for postoperative evaluation of endovascular abdominal aortic aneurysm repair. *J. Vasc. Surg.* **37**, 1142 (2000).

[21] H.E. Garret, A.H. Abdullah, T.D. Hodgkiss, and S.R. Burgar, Intravascular ultrasound aids in the performance of endovascular repair of abdominal aortic aneurysm. *J. Vasc. Surg.* **37**, 615 (2003).

[22] M.L. Raghavan and D.A. Vorp, Toward a biomechanical tool to evaluate rupture potential of abdominal aortic aneurysm: identification of a finite

strain constitutive model and evaluation of its applicability. *J. Biomech.* **33**, 475 (2000).

[23] S. Spring, B. van der Loo, E. Krieger, B.R. Amann-Vesti, V. Rousson, and R. Koppensteiner, Decreased wall shear stress in the common carotid artery of patients with peripheral arterial disease or abdominal aortic aneurysm: Relation to blood rheology, vascular risk factors, and intima-media thickness. *J. Vasc. Surg.* **43**, 56 (2006).

[24] T. Kenner, H. Leopoldz, and H. Hinghofer-Szalkay, The continuous high-precision measurement of the density of flowing blood. *Pflügers Arch.* **370**, 25 (1977).

[25] A.E. Green and W. Zerna, *Theoretical Elasticity.* University Press, Oxford (1954); Dover, New York (1992).

[26] M.A. Biot, Surface instability of rubber in compression. *Appl. Sci. Res.* **A12**, 168 (1963).

[27] M.A. Biot, *Mechanics of Incremental Deformations.* John Wiley, New York (1965).

[28] J.N. Flavin, Surface waves in pre-stressed Mooney material. *Q. J. Mech. Appl. Math.* **16**, 441 (1963).

[29] A.J. Willson, Plate waves in Hadamard materials. *J. Elasticity* **7**, 103 (1977).

[30] P. Chadwick and D.A. Jarvis, Surface waves in a pre-stressed elastic body. *Proc. Roy. Soc. Lond. A* **366**, 517 (1979).

[31] Lord Rayleigh, On waves propagated along the plane surface of an elastic solid. *Proc. Lond. Math. Soc.* **17**, 4 (1885).

[32] M. Braun, Rayleigh waves in a prestressed neo-Hookean material. *Proc. IUTAM Symp. on Nonlinear Deformation Waves* (U. Nigul and J. Engelbrecht, Eds.) Springer-Verlag, Berlin (1983).

[33] M.A. Dowaikh, Surface waves propagating in a half-space of neo-Hookean elastic material subject to pure homogeneous strain. *Int. J. Non-Linear Mech.* **35**, 211 (2000).